Orbital ordering in perovskites

Z. Jirák, Institute of Physics, Prague

1. Introduction

Transition metal oxides exhibit fascinating spectrum of physical properties depending on whether the d-electrons are localized on individual transition metal sites or are delocalized throughout the solid. Special attention attract systems with cations in the orbitally degenerate state, where preferential occupation of specific d-orbitals can lead to the development of a long-range ordered pattern. This phenomenon, referred as orbital ordering, makes the bonding between the cations in the oxides strongly directional depending on the kind of the occupied orbitals and their mutual orientation, which further influences magnetic interactions and electron transport.

Prototypical cases for perovskites are $LaVO_3$ (t_{2g} electron system) and LaMnO3 (e_g electron system). In both cases the quantum mechanical wavefunction of an electron, bound to the atomic nucleus by the Coulombic force, is characterized by an anisotropic distribution of density. The ordered configurations are notoriously known and consist of a staggered $t_{2g}=d_{xy}$, d_{yz}, d_{zx} and $e_g=d_{3z2-r2}$, d_{x2-y2} orbitals (see Fig.).

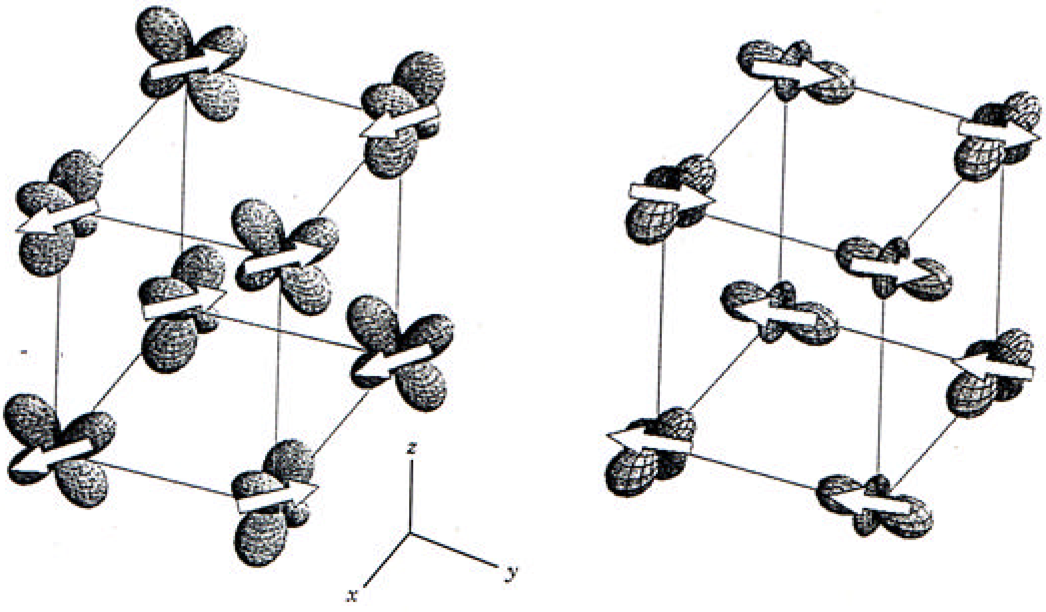

Fig. Orbital and spin patterns in $LaVO_3$ (left) and $LaMnO_3$ (right).

More interesting situation occurs in perovskites with transition metal cations in fractional valency. They are susceptible to charge ordering that coexists with the orbital ordering. This is best studied in manganates and different variants of the Mn3+/Mn4+ (1:1), (1:2) and (1:3) order were largely discussed during our previous meetings.

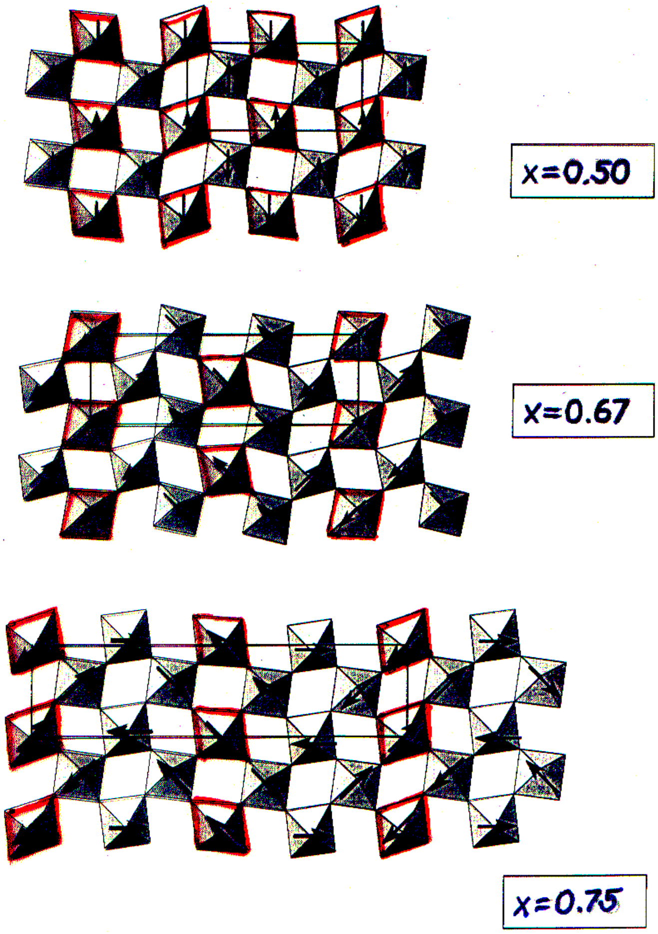

Fig. Charge order and magnetic arrangements in $Pr_{1-x}Ca_xMnO_3$. (In the next layer the spins are reversed.)

2. Orbitally degenerate ion in the isolated octahedron

An example of the doubly degenerate ion is Mn^{3+}. Its $3d^4$ electronic configuration can be viewed as one e_g electron moving in the central field of nucleus and effective potential of the occupied t_{2g} level and core electrons.

In the orbitally disordered case, the state of this electron is described as an incoherent mixture of the two quantum wavefunctions of the e_g electron. Their population is equal, defined by the density matrix

$$\mathrm{diag}(w1=1/2,w2=1/2) \equiv \begin{pmatrix} ½ & 0 \\ 0 & ½ \end{pmatrix}$$

in our choice of basis functions $\varphi_1=d_{3z2-r2}$, $\varphi_2=d_{x2-y2}$ or any other one $\psi_1=a_1\varphi_1+a_2\varphi_2$, $\psi_2=b_1\varphi_1+b_2\varphi_2$ (the eigenstates remain undefined in the orbitally disordered state).

Upon the ordering process, the density matrix acquires generally a non-diagonal form in the given basis, and its diagonalization determines what are the eigenstates and their temperature dependent populations. Finally, the mixed quantum state may be transformed to a pure quantum state with specified ground state of population 1 and excited state of population 0 (i.e., a complete orbital polarization). The character of these eigenstates is given by two classical quantities, the density distribution $\psi\psi^*$ and current-flow distribution in the electron cloud $\hbar/2m(\psi\nabla\psi^*-\psi^*\nabla\psi)$. It is seen immediately that for real-valued wavefunctions (up to some constant factor) there are no current flows in the electron cloud while the complex values of wavefunctions generally signal a presence of currents corresponding to dipole (orbital momentum) or to some multipole distribution.

One may suppose that eigenfunctions can be combined with any (complex-valued) coefficients a_1, a_2, b_1, b_2 but in fact the symmetry properties of the density matrix under operations of the octahedral point group O_h strongly limit the possibilities. Density matrix is transformed in the same way as the products $\psi_i\psi_j^*$, i.e. according to representation

$$E_g^2 = A_{1g}+E_g+A_{2g}.$$

The reduction of E_g^2 expresses a separation of the density matrix to a constant (cubic symmetric) part associated with the unit representation A_{1g} and two different temperature dependent parts that are associated with the two-dimensional irreducible representation E_g and one-dimensional representation A_{2g}.

In the crystal, the space group operations transpose the local orbital states but do not mix E_g and A_{1g} parts. This means that the symmetry allowed orbital configurations combine only the E_g or A_{2g} parts of local density matrices, which leads to two distinct types of ordering (Table I).

Z. Jirak, PRB 46, 8725 (1992)

GROUP-THEORETICAL APPROACH TO ORBITAL ORDERING . . .

TABLE I. Ordered local states based on the e_g electron orbitals.

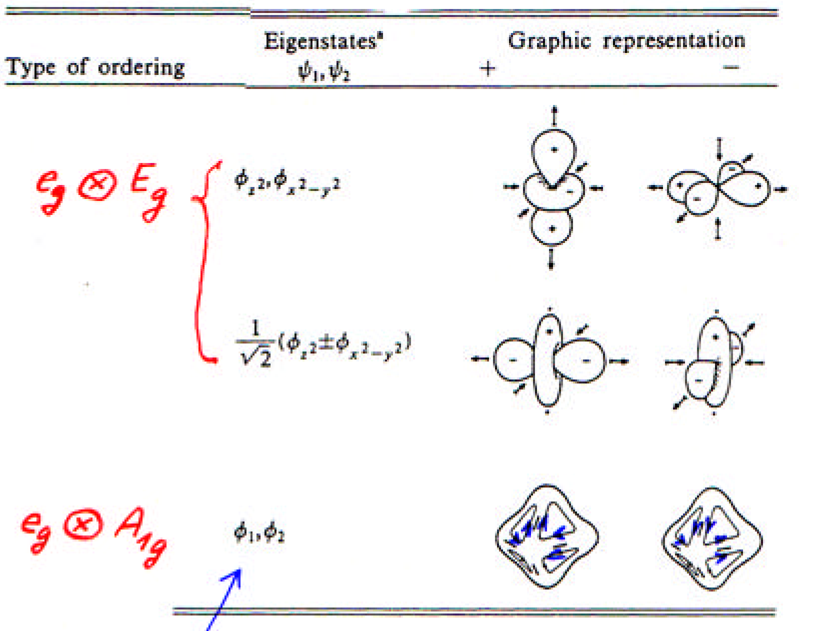

Type of ordering	Eigenstates^a ψ_1,ψ_2	Graphic representation +	−
$e_g \otimes E_g$	$\phi_{z^2},\phi_{x^2-y^2}$		
	$\frac{1}{\sqrt{2}}(\phi_{z^2}\pm\phi_{x^2-y^2})$		
$e_g \otimes A_{1g}$	ϕ_1,ϕ_2		

$$\phi_1 \sim \varepsilon x^2 + \varepsilon^2 y^2 + z^2 = \phi_2^* \quad (\varepsilon = e^{2\pi i/3})$$

The E_g type of orbital ordering is associated with the onset of noncubic electron distribution that can be expressed by two components – tetragonal and orthorhombic. If d_{3z2-r2} is the ground state, the electron density is enhanced in the z-axis (positive change) and decreased in xy plane (negative change). This is coupled with the tetragonal elongation of the octahedron (distortion mode Q_3, the most common type of Jahn-Teller effect in E_g ions). The complementary state d_{x2-y2} reverses the sign of the density change, and is coupled with the tetragonal contraction (distortion $-Q_3$) . The orthorhombic distortion $\pm Q_2$ is associated with eigenstates $1/\sqrt{2}(d_{3z2-r2} \pm d_{x2-y2})$. What is specific for the E_g type of ordering is a possible stabilization of any linear combination of wavefunctions $\cos\alpha/2\ d_{3z2-r2} + \sin\alpha/2\ d_{x2-y2}$ (i.e. with real coefficients !). The associated distortion has than two components $\cos\alpha\ Q_3 + \sin\alpha\ Q_2$ that play a role of classical order parameters.

The other type A_{2g} of the orbital polarization is characterized by a cubic distribution of electron density with a quadrupole magnetic moment due to currents depicted in Table I. Two complementary states (+ and -) are distinguished by opposite current flows. At this moment the occurrence of such kind of static orbital polarization is rather hypothetical even if Van der Brink and Khomskii recently considered such possibility.

The behaviour of triply degenerate ions is more complex. An example is octahedrally coordinated trivalent V with two 3d-electrons (or one hole) in the t_{2g} level and Ti with one 3d-electron. Its basis functions are d_{xy}, d_{yz} and d_{zx}. Under the requirement that the orbital polarization should tend to a pure quantum state (not to an incoherent mixture of two!), only discrete states are allowed. There is a possibility for $t_{2g}xE_g$ Jahn-Teller (JT) effect with stationary states d_{xy}, d_{yz} and d_{zx}, stabilized by tetragonal contraction ($-Q_3$) or elongation (Q_3) along three main axes (Table II). Another possibility is the $t_{2g}xT_{2g}$ JT effect with four stationary states that correspond to an elongation of electron density along different body diagonals and are coupled with trigonal distortions of the octahedron (combinations of Q_4, Q_5 and Q_6 modes belonging to the T_{2g} representation).

TABLE II. Ordered local states based on the t_{2g} electron orbitals.

Type of ordering	Eigenstates	Graphic representation
$t_{2g} \otimes E_g$	ϕ_{xy} ϕ_{yz} ϕ_{zx}	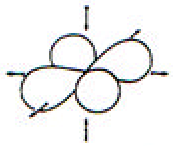 [001] or [100] or [010]
$t_{2g} \otimes T_{2g}$	$\frac{1}{\sqrt{3}}(\phi_{xy}+\phi_y z+\phi_{zx})$ $\frac{1}{\sqrt{3}}(\phi_{xy}-\phi_{yz}-\phi_{zx})$ $\frac{1}{\sqrt{3}}(\phi_{xy}-\phi_{yz}+\phi_{zx})$ $\frac{1}{\sqrt{3}}(\phi_{xy}+\phi_{yz}-\phi_{zx})$	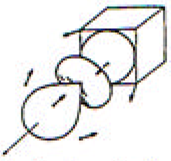 $[111]$ or $[1\bar{1}\bar{1}]$ or $[\bar{1}1\bar{1}]$ or $[\bar{1}\bar{1}1]$

Tables I and II show the density change upon the ordering while the density itself depends on distribution of all 3d electrons. For the configuration $3d^2$ for V^{3+}, $3d^4$ for Mn^{3+} and $3d^6$ for the intermediate-spin

Co^{3+}, the total density is shown in Fig. It should be noted to the orbitally ordered states that the complete polarization need not to be achieved because the real degree of polarization is an equilibrium of energy gain by the removal of the degeneracy and loss of elastic energy due to distortion. The charge distribution will be then less asymmetrical.

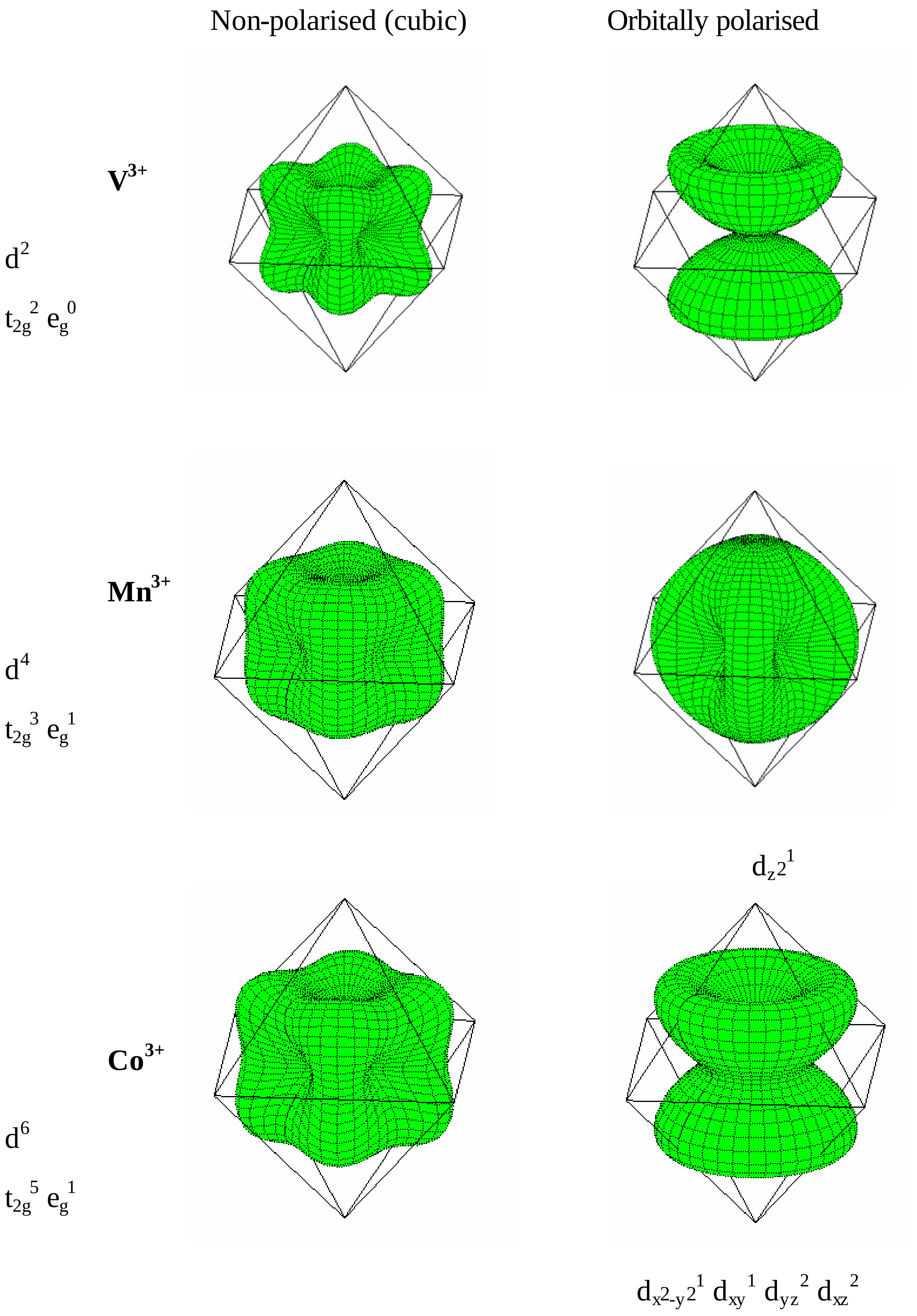

3. Jahn-Teller effect in crystals

The interesting property of crystals, concentrated in JT ions, is the occurrence of long range or so-called cooperative orbital ordering. The forces responsible for this ordering are long range acting elastic interactions of local JT distortions (these are surely decisive for ferrodistortive JT ordering in hausmanite Mn_3O_4), electron exchange interactions (probably primary in antiferrodistortive $LaMnO_3$ and other manganites) and others. The physical background of the cooperative JT effect was discussed in detail by Kugel and Khomskii in their early works and recently.

Concentrated JT systems – cooperative orbital ordering

Origin:

a) elastic interactions of local JT distorsions

b) interactions of electron-exchange type

c) electric dipole-dipole interactions, etc.,

Kugel and Khomskii,
Sov. Phys. – Solid State 15 (1973) 2230
Sov. Phys. – JETP 37 (1973) 725
Sov. Phys. – Uspekhi 25 (1982) 231
and recent works

Determination of coop. JT arrangements

a) trial and error

b) diffraction experiments

c) group-theoretical analysis
PRB 35 (1987) 5437
46 (1992) 8725
Physica B 183 (1993) 96

The orbital ordering pattern is generally deduced from the structural determination or can be predicted intuitively. There is, however, a more systematic way in the search of possible orbital configurations, that is based on the investigation how local orbital states in the crystal transform under space group symmetry operations. Then the configurations (with zero or nonzero wavevectors) are characterized with irreducible representations of given space group. This is a procedure analogical to the representation analysis of spin arrangements, well known for specialists in neutron diffraction. In the case of spins, one deals with transformation of classical axial vectors while in the case of orbitals with the transformation of density matrices. Using a more rigorous quantum-mechanical language, the problem of order-disordered transitions was recently treated in a review article of Izyumov and Syromyatnikov, Phase Transitions 66, 23 (1998).

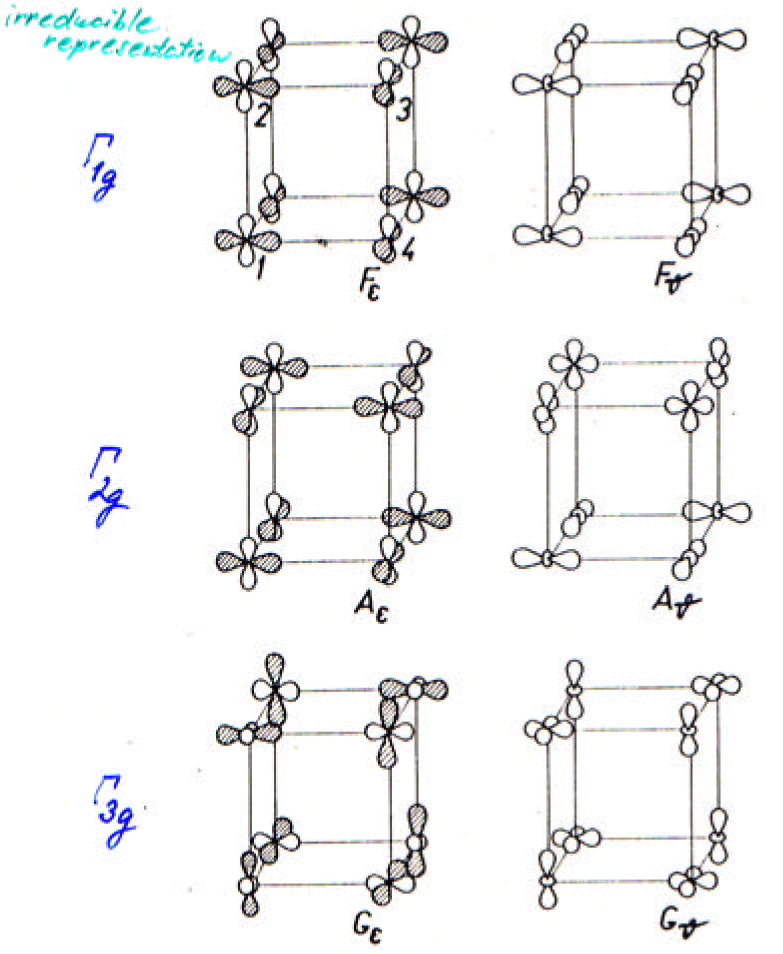

FIG. 2. Low-energy orbital configurations in orthoperovskites. (In orthorhombic ϵ states the long axis is depicted by the hatched lobes, the medium axis by the open ones. Small lobes along the shortest axis are not marked.)

for $\vec{k}=0$

Z. Jirak, PRB 35, 5437 (1987)

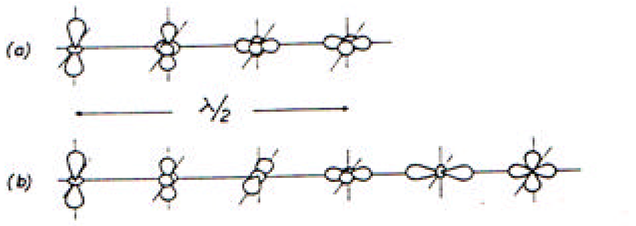

FIG. 10. Jahn-Teller wave (a) and spiral (b) for $\mathbf{k} \sim \frac{1}{6}\mathbf{b}_1$.

4. Perovskite systems diluted in JT ions

If the JT states are diluted in the crystal as in the case of mixed Mn^{3+}/Mn^{4+} valency, two cases might be distinguished. First, the conducting manganates with partially occupied σ^* band where in analogy to JT effect similar tendency to removal of orbital degeneracy exists (Peierls instability). To the second case belong systems with tendency to localization, as charge ordered insulators of the antiferromagnetic CE type or much less understood, badly conducting FM systems with formation of stripes of different electron density or more complex ordered patterns.

In the studies of charge ordered manganites, the interest is oriented to the investigation of various time and length scale fluctuations and their role in physical properties. It was found that long-range stable CO/OO becomes a short-range one when doping systems at Mn sites by other metals like Cr. In such case, competing FM or pseudo CE type AFM can be induced in expense of common CE type AFM in the parent compound. Existence of long-ranged strains, evidenced recently by Caen group in their synchrotron radiation and neutron diffraction studies of $Pr_{0.5}Ca_{0.5}Mn_{0.97}Ga_{0.03}O_3$ (C. Yaicle et al.), sheds light on the nature of such phase separated state. Similar strong effects occur also in half-doped manganates with large size mismatch in the large-cation sites, like $Ln_{0.5}Ba_{0.5}MnO_3$.

As to the charge separation effects in systems governed by FM interactions, two examples may be mentioned – $Pr_{0.5}Sr_{0.5}MnO_3$ and $La_{0.84}Sr_{0.16}MnO_3$. The first system is an A-type antiferromagnet below 140 K. The compound exhibits substantial conduction in the FM plane, facilitated by the d_{x2-y2} orbital polarization. Recent structural studies reveal, however, a superstructure with wavevector q=1/3 r.l.u. that can be interpreted as an alternation of hole-poor and hole-rich ribbons of manganese ions (Fig.).

Kajimoto et al., PRB 66 (2002) 180402

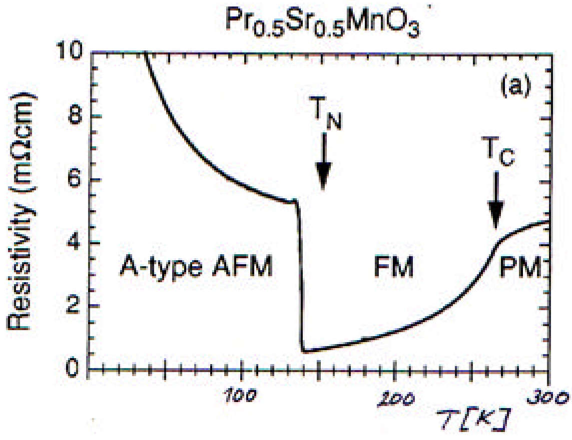

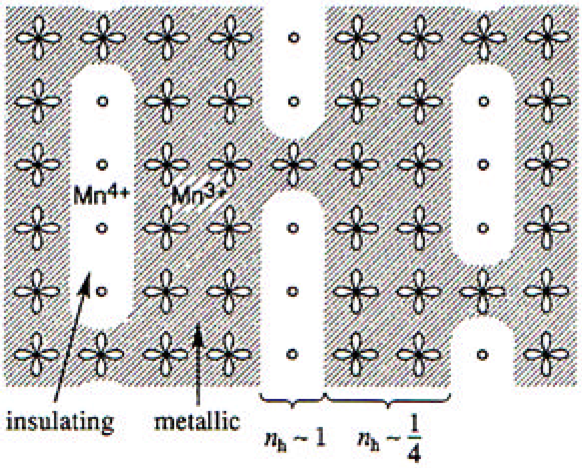

FIG. 4. Schematic illustration of the charge order and orbital order with $q=1/3$ r.l.u. Cloverleaf symbols represent the $d(x^2-y^2)$ orbitals. n_h denotes the hole concentration within the Mn^{4+} stripe or the Mn^{3+}-like matrix.

$La_{0.84}Sr_{0.16}MnO_3$ (average Mn valency 3.16) is ferromagnet below 250K. At 160 K, another transition is evidenced by an increase of resistivity. Small anomaly is also observed in FM moment. The NMR signal [Savosta *et al*. PRB 67, 100411 (2003)] measured at low temperatures showed a complex profile that could be separated into two motionally narrowed lines with intensity ratio 1:3 (Fig). The difference in resonance frequencies allowed to estimate that the less populated Mn species correspond to valency 3.35 (hole-richer sites) and more populated ones to 3.10 (hole-poorer sites).

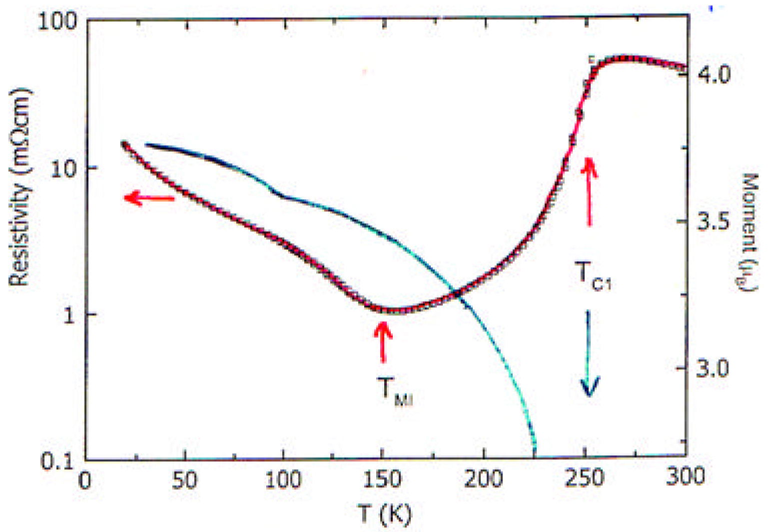

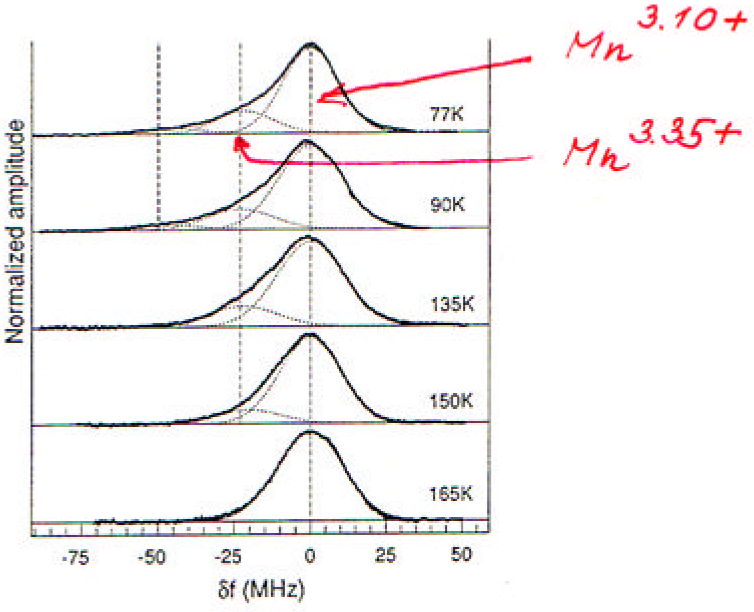

FIG. 4. $La_{0.84}Sr_{0.16}MnO_3$. The fit (full curve) of the NMR spectra (points). The spectra were shifted so that the maxima of their amplitudes coincide.

In the cooperation with JINR in Dubna we have performed a single crystal neutron diffractometry and confirmed a well ordered superstructure. The superstructure reflections can be indexed as [h=half-integer, k=half-integer, l] with respect to the orthorhombic cell of Pbnm symmetry. The study is not finished yet, because of severe effects of primary extinction in the diffraction that make quantitative analysis difficult. However, the progressive increase of superstructure reflections with increasing h=half-integer, k=half-integer defines with certainty that the structure displays systematic oxygen shifts shown by arrows in Fig. This is consistent with orbital order at the majority, hole-poor sites as depicted, while the minority, hole rich sites form conducting chains along the c-axis.

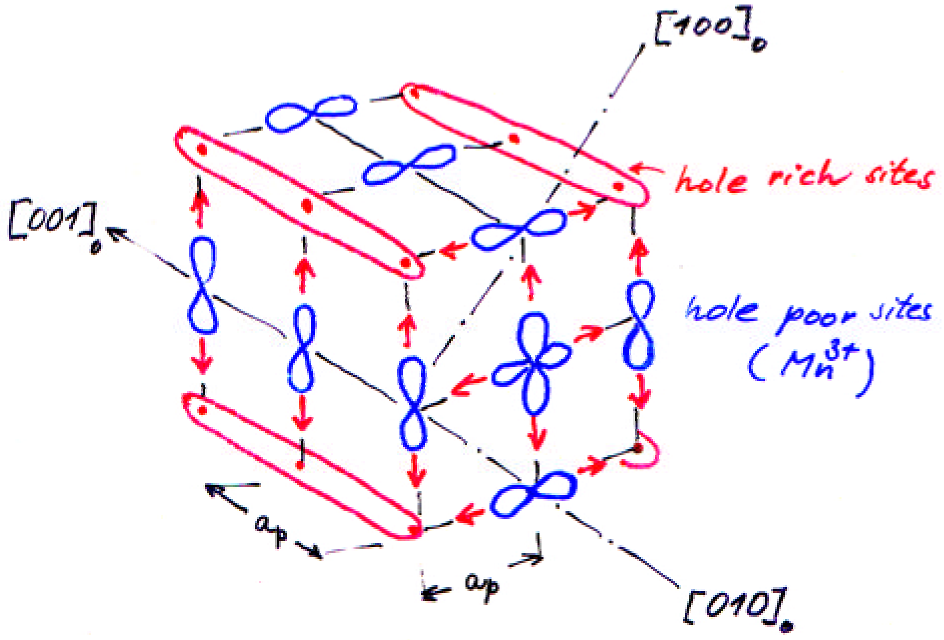

Fig. Charge and orbital order in La$_{0.84}$Sr$_{0.16}$MnO$_3$.